Protection of Hematite Photoelectrodes by ALD-TiO_2 Capping

T. Imrich[a], R. Zazpe[b,c], H. Krýsová[d], Š. Pausová[a], F. Dvorak[b], J. Rodriguez-Pereira[b], J. Michalicka[c], O. Man[c], J.M. Macak[b,c], M. Neumann-Spallart[a], J. Krýsa[a]*

[a] Department of Inorganic Technology, University of Chemistry and Technology Prague, Technická 5, 16628 Prague 6, Czech Republic

[b] Center of Materials and Nanotechnologies, Faculty of Chemical Technology, University of Pardubice, Nam. Cs. Legii 565, 53002 Pardubice, Czech Republic

[c] Central European Institute of Technology, Brno University of Technology, Purkyňova 123, 61200 Brno, Czech Republic

[d] J. Heyrovský Institute of Physical Chemistry of the Czech Academy of Sciences, Dolejškova 2155/3, 182 23 Prague 8, Czech Republic

Abstract

Iron (III) oxide, in the form of hematite (α-Fe_2O_3), is a n-type semiconductor which is photoactive in the visible. Therefore, use in photoelectrocatalysis and photoassisted water electrolysis has been suggested. For such implementations, stability of contacts with liquid phases is mandatory. Hematite is stable in alkaline media but less stable in acidic media. The possibility of hematite protection against chemical dissolution in acidic media by thin capping layers of TiO_2, deposited by Atomic Layer Deposition (ALD) was thus investigated. Hematite layers, as obtained in this study by aerosol pyrolysis (AP) were rough and porous. ALD is very useful in applying conformal films to such structures. The nominal thicknesses of the TiO_2 ALD coatings were 0.5, 2 and 7.5 nm. The presence of the TiO_2 coatings was evidenced by X-ray photoelectron spectroscopy, high-resolution transmission electron microscopy (HR-TEM) and scanning TEM coupled with energy dispersive X-ray (EDX) spectroscopy. HR-TEM analyses revealed that the TiO_2 capping layers were amorphous and conformal. Exposure of uncovered hematite layers to 1 M sulfuric acid led to a nominal dissolution rate of 0.23 nm/h which was halved when a TiO_2 ALD coating (7.5 nm thin) was applied. Due to mismatch of the valence band positions of the two semiconductors, photocurrents were strongly diminished as the capping layer thickness was increased. Post-calcination of as deposited ALD films on hematite results in an increase of photocurrent, which only exceeded photocurrents of pristine hematite when the ALD thickness was not more than 0.5 nm.

keywords: hematite, TiO_2 capping layer, chemical dissolution, ALD, XPS

email: josef.krysa@vscht.cz (J. Krýsa)

Introduction

Corrosion protection of semiconductor materials is a topic of vivid interest. In addition, in some cases, *photo*corrosion takes place. With n-type semiconducting oxides, cases with fair resistance against photocorrosion can be found, which may be further improved if continuous operation in photochemical processes is envisaged. One of the recently intensively studied n-type semiconducting oxide is hematite (α-Fe_2O_3), due to its photoactivity in the visible. Therefore, its use in (solar powered) photoelectrocatalysis and photoassisted water electrolysis has been suggested.

Hematite is stable in alkaline media but less stable in acidic media [1]. Extending the radius of action of this material can be envisaged by strengthening its corrosion resistance by capping with a thin layer, such that light absorbance is not hindered. Insulating or wide bandgap semiconducting oxides are preferred material choices for a capping layer. The requirements necessary for a good protection are i) conformal coating and ii) sufficiently low electrical resistance for enabling charge transport through the capping layer.

The structure (roughness, porosity) of both, the underlayer and the capping layer is decisive for conformal coating, i.e. complete shielding of the semiconductor layer from the electrolyte. If conformal coating by a capping layer is achieved, the problem of hindrance of charge carrier transport from the underlying semiconductor to the electrolyte arises. With very thin films, even if insulating, tunneling can overcome this limitation to some extent. Thicker semiconductor films would need favorable matching of bands. This situation can rarely be found, and notches, spikes and kinks arise in the band alignment of a junction of two semiconductors, especially if the capping material has a large bandgap [2]. In this case, again, the capping film must be very thin (around 1 nm) in order to allow for tunneling [3].

Hematite layers, as obtained by aerosol pyrolysis have non-negligible roughness and porosity[4]. Previous work has succeeded to partially stabilize hematite films (as to photocorrosion) by capping with TiO_2 by spray pyrolysis [5].

In the present study, the possibility of protection of hematite electrodes against dissolution in acid by thin capping layers of TiO_2 using atomic layer deposition (ALD) is investigated. ALD is a well stablished deposition technique based on self-limiting gas-surface reactions. The chemical precursors are introduced in the reaction chamber in sequential alternating steps separated by purging steps using an inert gas [6]. Nowadays, ALD is the only method that enables homogeneous, pinhole free, continuous, and conformal coating of complex substrates with different porosity and pore size. A wide number of applications successfully utilized ALD by depositing (ultra)thin films of different nature. In particular, ALD is very useful for the deposition of anti-corrosion (ultra)thin films onto semiconductors with intrinsically poor stability in aqueous solutions [3]. Nevertheless, the deposited coating material must be appropriately selected not to inhibit two fundamental processes that strongly determine the performance of a semiconductor material i) light absorption and ii) charge carrier transfer through the layer. Therefore, materials with a wide band gap would not be detrimental for semiconductor light absorption, while ultrathin films ($\leq$ 2 nm) do not prevent electron tunneling.

In the last years various types of ZnO photoelectrodes have been coated with different materials, e.g., TiO_2 or Ta_2O_5, leading to a significant improvement of photocurrent stability [3, 7-9]. Regarding hematite photoelectrodes, there are many papers [10-14] about hematite/titania-based systems but the protection function of TiO_2 overlayers was not studied whereas most papers describe the aspect of surface passivation or minimizing of charge recombination due to the coverage by a TiO_2 layer.

Yang et al. [10] ascribed improvement of photocurrents of an ALD hematite film covered with TiO_2 for diminishing surface charge recombination. Li et al. [11] reported that as-deposited Fe_2O_3 (hydrothermal) was inactive but when TiO_2 coated samples were annealed, photocurrents were produced. However, this is no surprise as only after annealing crystalline hematite was present. Ahmed et al. [12] developed a facile solution method for the

modification of nanostructured hematite photoanodes with TiO_2 overlayers using a water based TiO_2 precursor (Ti bis(ammonium lactate) dihydroxide, TALH). Jeon et al. [13] used the same water based TiO_2 precursor as in [12] to load a ~3.5-nm-thick TiO_2 overlayer on hematite (α-Fe_2O_3) nanorod arrays. Wang et al. [14] used an ethanolic solution of tetrabutyl titanate (TBOT) for the deposition of a TiO_2 underlayer and overlayer on hematite nanorod films, followed by fast annealing. The TiO_2 underlayer and overlayer not only served as dopant sources for carrier density increase but also reduced charge recombination at the fluorine-doped tin oxide (FTO)/hematite interface and accelerated charge transfer across the hematite/electrolyte interface.

The intrinsic nature of as-deposited hematite films requires the addition of a suitable metal dopant. As shown in our previous work Sn doping of hematite photoelectrodes fabricated by aerosol pyrolysis increased photocurrents by one order of magnitude as compared to undoped films [4]. In this work TiO_2 films of different thicknesses, deposited by ALD, were explored as capping layers of Sn doped porous hematite photoelectrodes fabricated by aerosol pyrolysis for protection against chemical dissolution. Only two previous papers deal with ALD TiO_2 on hematite [10, 11] but none of them on active porous hematite. This is the first paper to report this.

Experimental

Iron (III) chloride and Sn (II) chloride, NaOH and H_2SO_4 were of analytical grade. Triply distilled water was used for the preparation of solutions.

Fluorine doped tin oxide coated 2 mm thick glass ("FTO", 7 Ω/□), obtained from Solaronix, was used as a substrate. Substrate pre-cleaning was done ultrasonically by degreasing with trichloroethylene followed by treatment with acetone, ethanol and water and drying in a stream of argon.

In aerosol pyrolysis (AP), a mist of the precursor solution was generated by ultrasound and directed by a stream of air onto the substrate which was fixed on a temperature regulated susceptor. Details of the apparatus have been described previously [15]. Deposition of thin films of hematite by aerosol pyrolysis has been described elsewhere [4].

Atomic layer deposition (ALD) was carried out using a TFS 200 tool (Beneq) at 300 °C using $TiCl_4$ (electronic grade 99.9998%, STREM) and Millipore deionized water (18 MΩ·cm) as the titanium precursor and the oxygen source, respectively. High purity N_2 (99.9999%) was the carrier and purging gas at a flow rate of 400 standard cubic centimeters per minute (sccm). Under these deposition conditions, one ALD cycle was defined by the following sequence: $TiCl_4$ pulse (500 ms) − N_2 purge (3 s) − water pulse (500 ms) − N_2 purge (4 s). TiO_2 coatings of different nominal thicknesses, namely, 0.5 nm, 2 nm and 7.5 nm, were deposited by applying 10, 40 and 150 ALD cycles, respectively.

The structural, morphological and optical properties of the deposited hematite films were determined by X-ray diffraction (X'pert Philips MPD with a Panalytical X'celerator detector using graphite monochromatized Cu-K_α radiation (wavelength 1.54056 Å)), field emission scanning electron microscopy (FE-SEM, Hitachi SEM FE 4800), profilometric thickness measurement (Dektak XT), UV-Vis absorption spectroscopy (Cary 100 and Mikropack NanoCalc 2000), and optical microscopy (Axio Scope A1, Zeiss).

The chemical composition of ALD TiO_2 coated AP hematite films was determined by X-ray photoelectron spectroscopy (XPS, ESCA 2SR, Scienta-Omicron) using a monochromatic Al-K_α source (1486.6 eV). The binding energy scale was referenced to adventitious carbon (284.8 eV) and the quantitative analysis was performed using sensitivity factors provided by the manufacturer. Depth profiling was performed using the Ar^+ cluster ion beam (GCIB 10s, IonOptika). The size, energy, and sample current of Ar^+ clusters was 500 ± 100 atoms, 10 keV, and 10 nA, respectively. The depth profile of the atomic concentration was determined based on the quantitative analysis of survey spectra obtained from sputtered

surfaces. Scanning transmission electron microscopy (STEM coupled to energy dispersive X-ray spectroscopy (EDX) and high resolution TEM (HR-TEM) were used for investigating the composition and crystallinity of the involved layers, respectively. A TEM TITAN Themis 60-300 (Thermo Fisher Scientific, The Netherlands) operated at 300 kV and equipped with a C_s-image corrector, a SUPER-X EDX detector and a high-angle annular dark-field (HAADF) STEM detector were used for this purpose. The TEM sample was employed in the form of thin cross sectional lamella prepared by focused ion beam (FIB) milling with a dual-beam microscope HELIOS NanoLab 660 (Thermo Fisher Scientific, Czech Republic).

The determination of the iron concentration in solution was carried out by inductively coupled plasma spectrometry (ICP) using an ICP-OES Optima 8000 (Perkin Elmer) machine.

Photoelectrochemical measurements were performed potentiodynamically using a Voltalab 10 PGZ-100 potentiostat and an Ag/AgCl or SCE reference electrode. Voltammetry was carried out under periodical (5 s light / 5 s dark) front side illumination of the electrolyte/electrode interface ("EE", through the electrolyte) or backside irradiation ("SE", through the substrate / electrode interface). Aqueous solutions of H_2SO_4 or NaOH were used as electrolytes. For the incident photon to current efficiency (IPCE) spectra, an Electrochemical Photocurrent Spectra CIMPS-pcs system (Zahner, Germany) with a TLS03 tunable light source was used. IPCE and polarisation measurements at single wavelengths were carried out using LED (light emitting diode) backside illumination (through the glass substrate) and a calibrated Hamamatsu S1337-1010BQ photodiode. For polychromatic experiments, a solar simulator (150 W Xe arc lamp (Newport) with an AM1.5G filter, irradiance 1 sun (100 mW/cm^2) was used.

Results and discussion

AP deposited hematite layers on FTO were rough and porous as seen by SEM and stylus profilometry (Fig. 1). The thickness of the sample of which the profilometric trace was around 600 nm (5 min. deposition time).

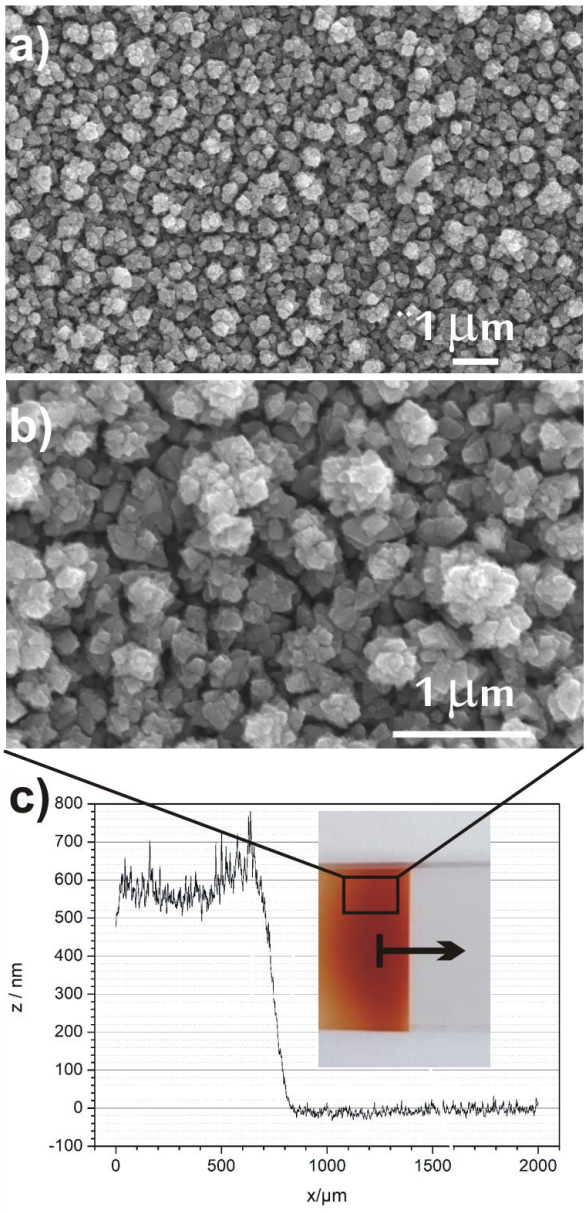

Fig. 1. a, b) SEM images of AP hematite film on FTO, c) profilometric trace; inset: photographic image of step over the edge of the hematite film on FTO. Precursor for AP: 0.05 mol/l $FeCl_3$, 0.5 mmol/l $SnCl_2$, deposition time: 5 min. at 650 °C.

TiO_2 capping layers of different nominal thickness were deposited by ALD. SEM pictures of AP hematite films with a capping TiO_2 layer looked almost identically to that in Fig. 1. Furthermore, XRD and grazing incidence XRD did not show any diffraction pattern stemming from TiO_2, due to the thinness of the capping overlayers (see Fig. S1 in Supplementary Information (SI)).

Nominal thickness was calculated from the number of deposition cycles – extrapolated from the deposition of TiO_2 on an atomically flat surface (Si). Based on previous work [16] it can be assumed that TiO_2 is conformally deposited even in the case of porous films. To confirm this, we performed STEM-EDX analysis. ~~However,~~ STEM-EDX revealed the presence and conformality of the ALD deposited capping TiO_2 layers and confirmed their thickness (Fig. 2a,b). HR-TEM (Fig. 2c,d,e) showed that the TiO_2 layer was amorphous. Based on our previous work, a certain thickness is needed to develop 3-D crystals, e.g. spray deposited anatase films of less than 50 nm were never crystallized, even when deposited at 470 °C [17]. Further HR-TEM results are shown in SI as Figs. S2 and S3 and Table S1, respectively.

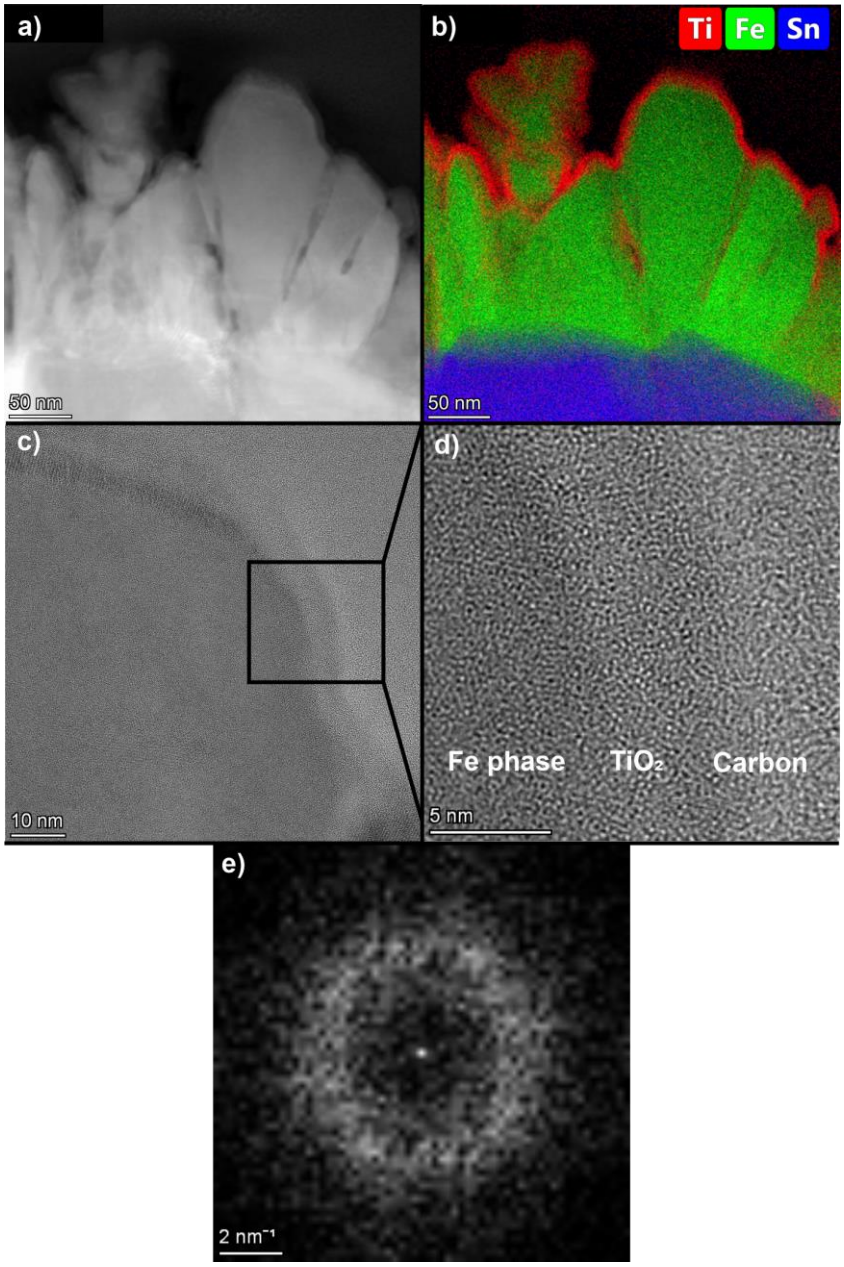

Fig. 2. (a) STEM-HAADF image of a cross-section of a hematite film with a TiO_2 capping layer, (b) EDX elemental color map showing the presence of elements of interest, i.e. Ti (red), Fe (green), Sn (blue), (c) TEM image of the inteface between the hematite film and ALD deposited TiO_2 capping layer, (d) detailed HR-TEM image of the same interface, (e) corresponding FFT pattern confirming the amorphous structure of the TiO_2 layer.

The results of XPS chemical analysis of a 7.5 nm thick TiO_2 capping layer coated on an AP hematite film are shown in Fig. S4 (in SI). In order to reveal the chemical composition of the TiO_2/hematite interface, the sample was depth profiled using repeated cycles of

sputtering by Ar_{500}^{+} clusters. The survey, Ti 2p, Fe 2p and O 1s XPS spectra of as deposited (black) and sputtered (blue) sample are shown in Fig. S4a-d, respectively. On the as-deposited sample shown in Fig. 3b, only the signal from TiO_2 ALD coating was detected with the Ti $2p_{3/2}$ peak found at 458.5 eV which corresponds to TiO_2 [18]. The lack of a signal from the AP hematite support manifests the conformality of the ALD TiO_2 coating. The survey spectrum revealed minor contamination by Si, Ca, N and the usual presence of adventitious carbon. N contamination could stem from the ALD process (N_2 physisorption during the N_2 purge cycles).

In order to reveal the chemical composition of the TiO_2/hematite interface, the sample used for XPS analyses in Fig. S4 was depth profiled using repeated cycles of sputtering by Ar_{500}^{+} clusters. The sputtering by Ar^{+} clusters resulted in the appearance of a signal from the AP hematite support (and of its dopant, Sn) accompanied by successive removal of surface contamination. The concentrations of Ti, Fe, Sn and oxygen are shown as depth profiles in Fig. 3. The nominal thickness of the TiO_2 layer was 7.5 nm, but as can be seen from the depth profiles, Ti persisted far beyond the depth of 20 nm. This proofs that the ALD process permitted to coat the hematite layer well within its porous structure.

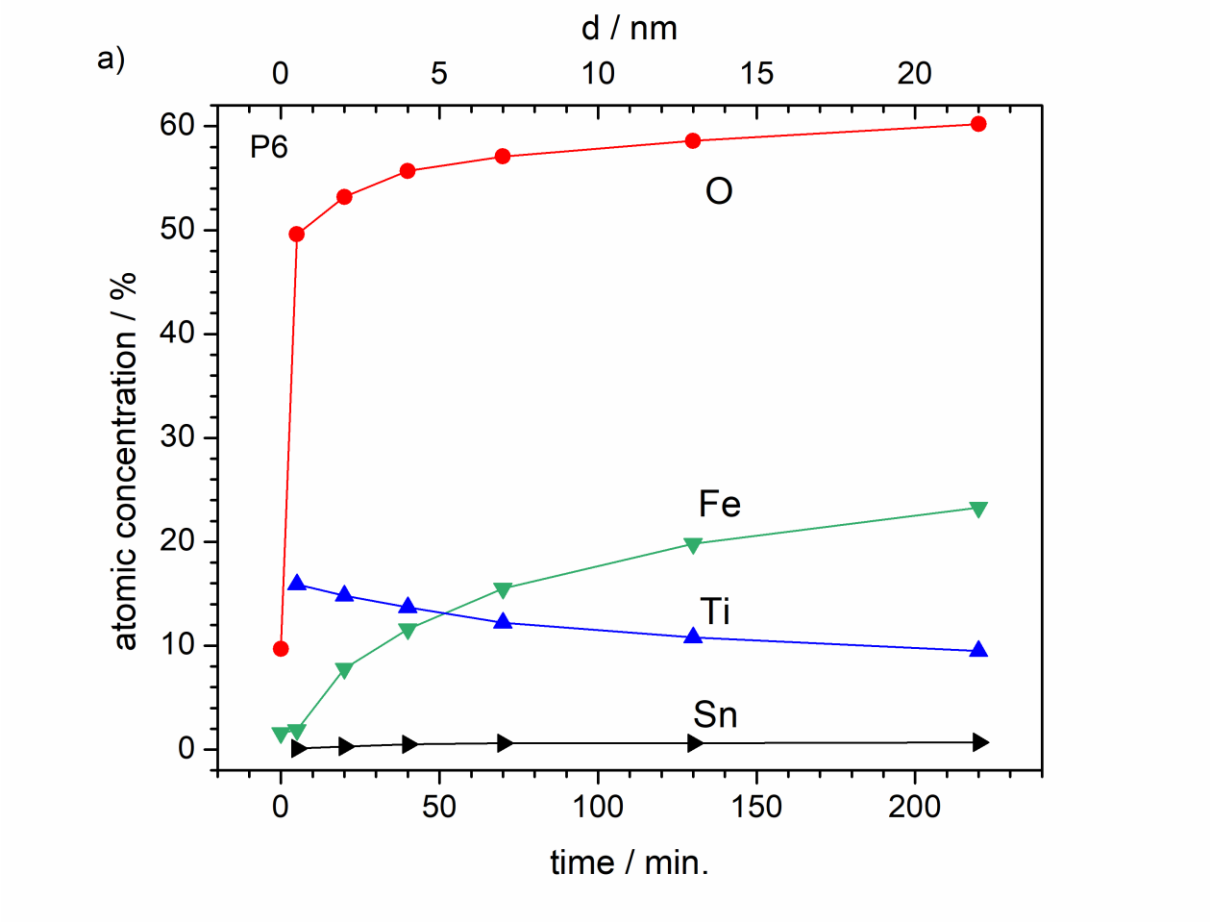

Fig. 3. The evolution of the atomic concentration of selected elements during depth profiling of as deposited (before H_2SO_4 treatment), nominal 7.5 nm TiO_2 capping layer on AP hematite films by an Ar^+ cluster ion source as determined from quantitative analysis of survey XPS spectra.

The Fe 2p spectrum from sputtered AP hematite shown in Fig. S4c (in SI) features the Fe $2p_{3/2}$ signal at 709.7 eV with the Fe $2p_{3/2}$ satellite at 715 eV which points to dominance of the Fe^{2+} oxidation state [19]. The presence of Fe^{2+} which is in contrast with the expected presence of Fe^{3+} can be attributed to sputtering induced damage of the surface region which is also evident in the Ti 2p spectrum of sputtered AP hematite with Ti^{3+} defect states around 457.5 eV (see Fig. S4b in SI) [18].

The O 1s spectrum of the as deposited sample displays two strong peaks. The one at 529.9 eV corresponds to oxygen bonded to metal (in this case only to titanium (TiO_2) [20, 21]). The one at 532.2 eV was assigned to adsorbed oxygen/surface -OH species [22, 23] (Fig.

S4d in SI). For a sputtered sample, the O 1s signal at 529.9 eV was attributed to oxygen bonded to titanium (TiO_2) and oxygen bonded to iron (Fe-O). It was not possible to differentiate between the two since the binding energies are very similar [19-21] and a signal associated with the remaining adsorbed oxygen was also observed (Fig. S4d in SI).

Fig. 4 shows that with increasing thickness of the capping TiO_2 layer the photocurrents are diminished. Only a very thin layer of 0.5 nm permits to retain a good part of the initial photocurrent. The photocurrent was completely suppressed for the 7.5 nm thick TiO_2 layer. A similar result was obtained for TiO_2 overlayers obtained by spray pyrolysis [5]. The observed effect can be ascribed to the hindrance of tunneling.

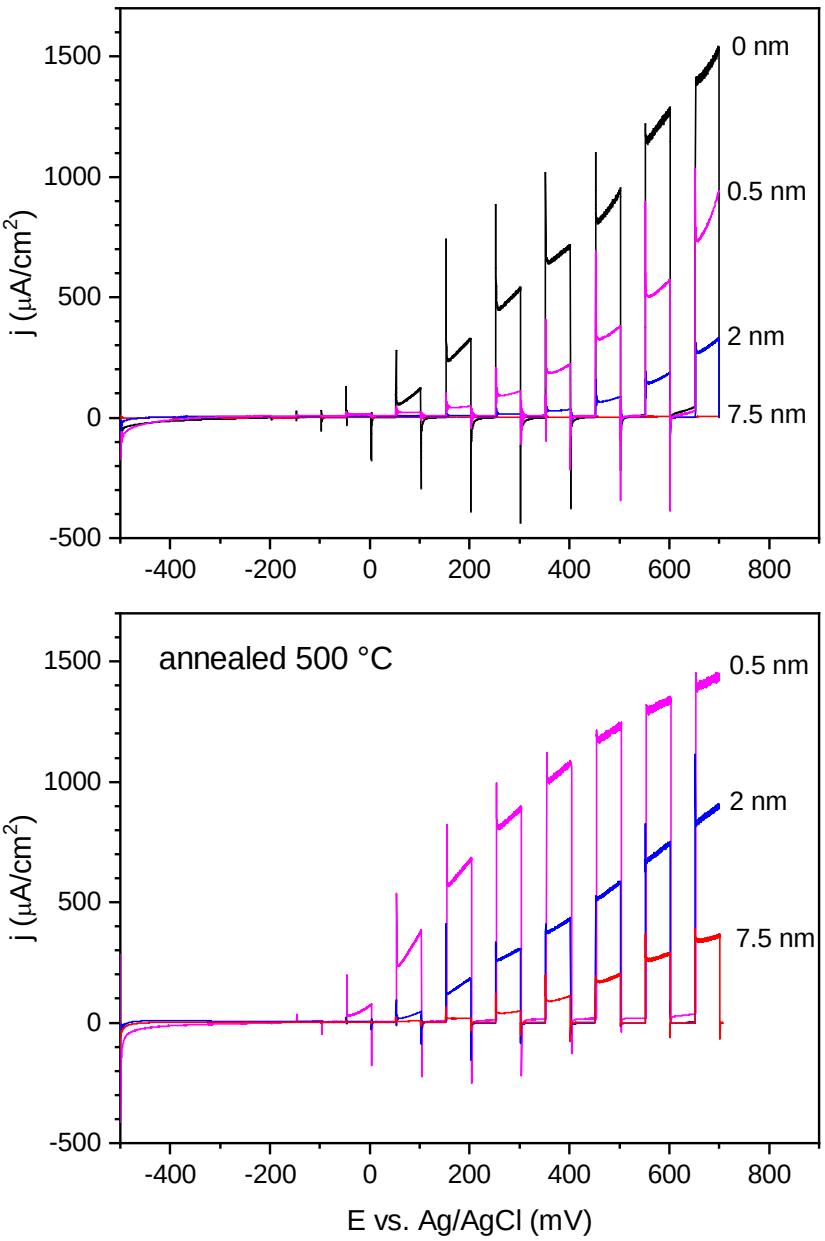

Fig. 4. Polarization curves of AP hematite films covered by ALD-TiO_2 of 0.5 nm, 2 nm, and 7.5 nm (upper graph). Annealed samples (500 °C, 30 min.) with 0.5 nm, 2 nm, and 7.5 nm thick TiO_2 films (lower graph). Precursor for AP: 0.05 mol/l $FeCl_3$, 0.5 mmol/l $SnCl_2$, AP-deposition: 5 min. at 650 °C. Precursor for ALD: $TiCl_4$. Electrolyte 1 M NaOH, scan rate +10 mV/s, light off and on interval 5 s, solar simulator.

The influence of post annealing in air (30 min. at 500 °C) of samples after TiO_2 deposition by ALD is also shown (Fig. 5). Photocurrents for all thicknesses of overlayers

increase. This may be due to crystallization at the post annealing temperature. The increase in photocurrents of annealed electrodes as also shown in Fig. 4 can be ascribed to the loss of the blocking function of TiO_2, due to increase in conductivity or due to partial delamination from the hematite electrode surface leading also to diminished corrosion resistance.

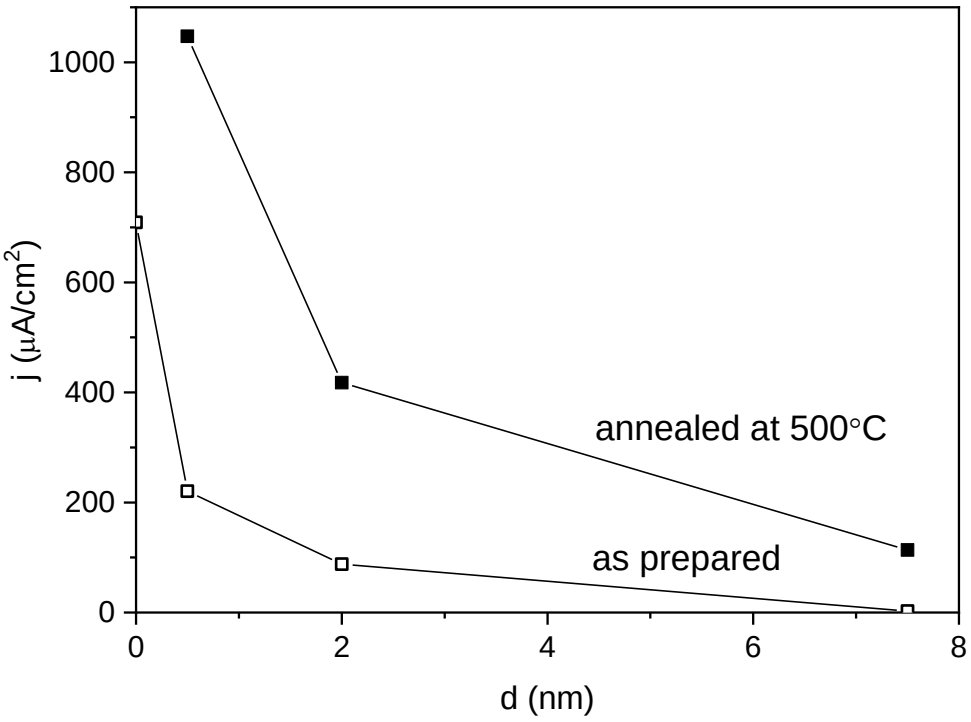

Fig. 5. Dependence of photocurrent density at 0.4 V of AP hematite films on FTO on coverage by ALD TiO_2 of thickness 0.5 nm – 7.5 nm (open squares) and after annealing at 500 °C for 30 min. (filled squares). AP: precursors 0.05 mol/l $FeCl_3$, 0.5 mmol/l $SnCl_2$, deposition: 5 min. at 650 °C. Precursor for ALD: $TiCl_4$. The connecting lines are used for eye guidance.

IPCE was recorded as a function of wavelength for front-side and back-side illumination (Fig. 6).

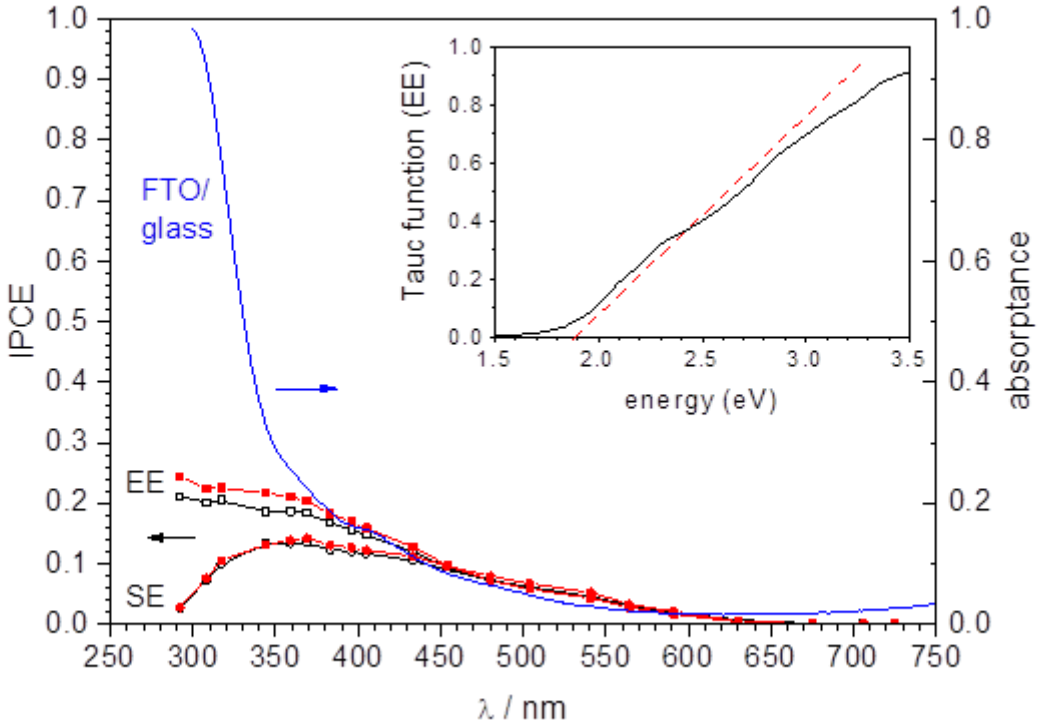

Fig. 6. IPCE at 0.4 V vs. Ag/AgCl, electrolyte 1 M NaOH, pure hematite (open symbols) and hematite + ALD TiO_2 0.5 nm, calcined at 500 °C (filled symbols). EE … illumination through the electrolyte, SE … illumination through the transparent substrate. Inset: Tauc function plot assuming an indirect transition.

The onset of photoactivity was found around 1.9 eV in accordance with the literature by extrapolation as shown in the inset of Fig. 6. The Tauc_function as defined by "(constant × absorbance × hν)$^{1/2}$" was replaced by (ln(1/(1-IPCE)) ×·hν)$^{1/2}$, and an example is shown for a sample of hematite + 0.5 nm ALD-TiO_2 annealed at 500 °C. The IPCE response for the annealed 0.5 nm capped sample is very similar to that of an as-deposited sample across the whole explored wavelength range, which is also reflected in the white-light response, Fig. 4. The decrease of IPCE in SE mode (irradiation from the substrate / electrode interface side) at lower wavelengths is because charge carriers formed far away from the interface with the electrolyte combine before reaching it due the short minority carrier diffusion length. Additional decrease of IPCE in SE mode at very low wavelengths is due to light absorption

by the conducting underlayer (FTO) and its support (glass). Absorptance of FTO/glass as a function of wavelength is also shown in Fig. 6.

Long term polarization under light

Pristine Sn doped hematite photoanodes and Sn doped hematite photoanodes covered by ALD TiO_2 layers were polarized under irradiation at a potential of 1.5 V vs. RHE in 1 M H_2SO_4. This potential corresponds to a potential 0.5 V vs. AgCl in 1 M NaOH which is lower than the dark current onset potential so that dark currents are negligible. Fig.7 shows the comparison of a hematite photoanode and one covered by a 2 nm thick ALD TiO_2 layer. It can be seen that coverage with 2 nm TiO_2 reduces the photocurrents considerably. The photocurrent decay rates of uncovered hematite and hematite covered with 2 nm TiO_2 are identical.

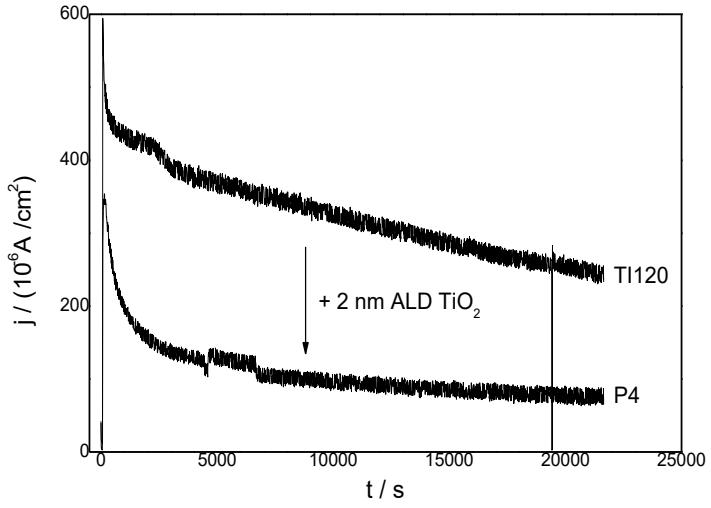

Fig. 7. Photocurrent density vs. time at 1.5 V *vs.* RHE for pristine hematite (TI120) and hematite + 2 nm ALD TiO_2 (as deposited) (P4). Electrolyte 1 M H_2SO_4, solar simulator.

Further attention was given to the influence of post-calcination of hematite covered by TiO_2 ALD films. As shown in Fig. 5, capping with TiO_2 results in a decrease of anodic photocurrent, post annealing resulted in photocurrent improvement and for 0.5 nm increased

photocurrents compared to pristine hematite were observed. A similar situation can be seen in the case of polarization in acidic media. Fig. 8 shows the current density as a function of time under irradiation of a hematite photoanode covered by 0.5 and 2 nm ALD TiO_2 layer annealed at 500 °C for 30 min. An improvement of the photocurrents of an uncovered hematite electrode (compare with data in Fig. 7) by applying a 0.5 nm ALD TiO_2 layer followed by annealing of this structure, can be seen as well as a slower photocurrent decay compared to pristine hematite. In comparison to 2 nm, the initial photocurrent is higher but the decay is faster.

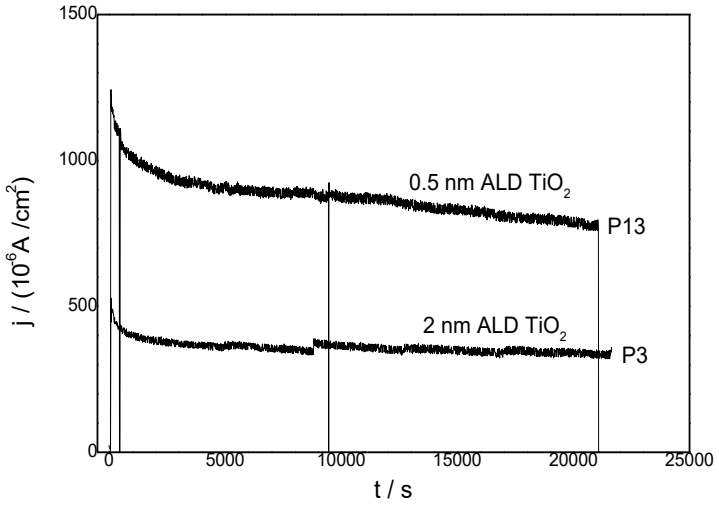

Fig. 8. Photocurrent density vs. time at potential 1.5 V *vs.* RHE for hematite AP + 2 nm ALD TiO_2 (annealed) (P3) and hematite AP + 0.5 nm ALD TiO_2 (annealed) (P13). Electrolyte 1 M H_2SO_4, solar simulator.

Chemical dissolution studies.

Fe_2O_3 is known to be stable in alkaline media but can be dissolved at low pH [1]. In order to check this reaction, electrodes were exposed to 1 M sulfuric acid for up to 7 days and the electrolyte analyzed afterwards by ICP. The thickness decreased on average by 0.23 nm/h. This nominal dissolution rate refers to a surface area of 1 cm^2 (the geometric area of the electrodes). In reality, the surface area is much larger, as the material is in the form of an open

porous network (see Fig. 1a,b). Therefore, the actual dissolution rate is much lower than 0.23 nm/h. ALD capping TiO_2 layers reduced the nominal loss rate to 0.12 nm/h. However, full protection was not achieved due to partial dissolution of TiO_2 as indicated by the XPS depth profiles (Figs. 3 and 8).

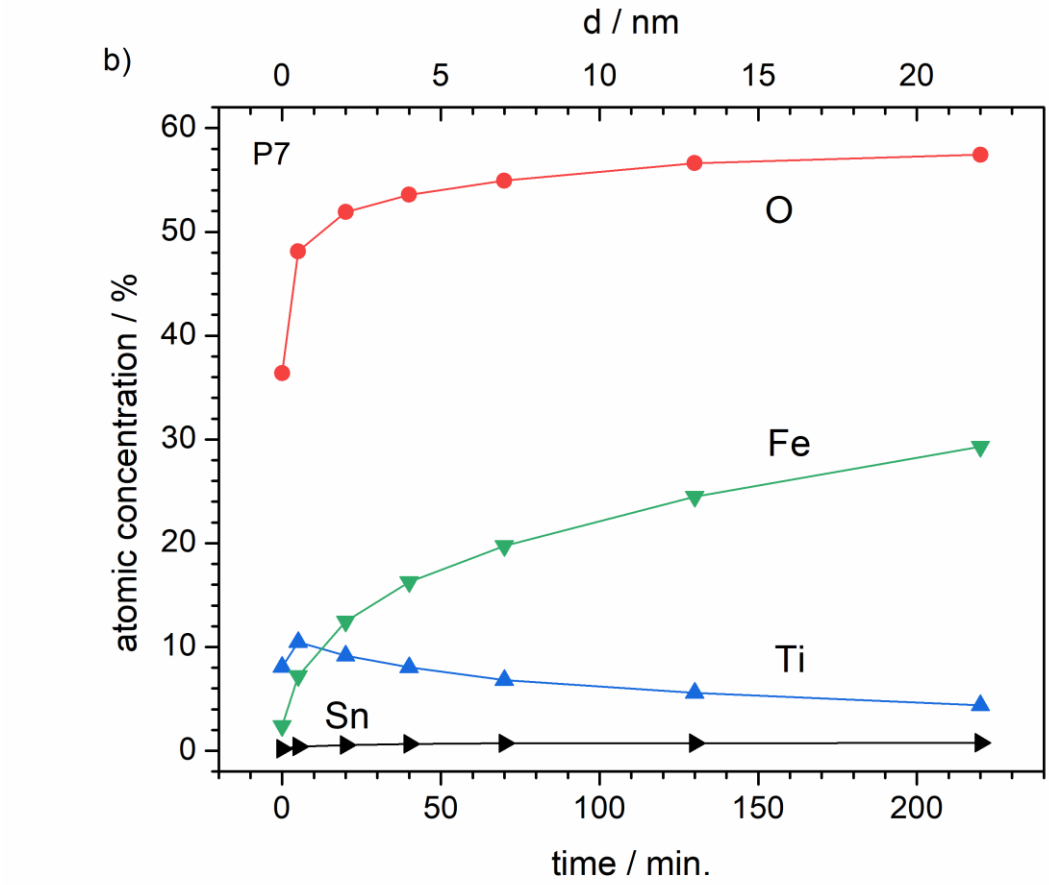

Fig. 8. The evolution of the atomic concentration of selected elements during depth profiling of nominal 7.5 nm TiO_2 capping layer on AP hematite films (after immersion in 1 M H_2SO_4 for 7 days) by an Ar^+ cluster ion source as determined from quantitative analysis of survey XPS spectra.

A sample of AP hematite films covered by a 7.5 nm thick TiO_2 capping layer and exposed in 1 M H_2SO_4 for 7 days at room temperature was depth profiled using repeated cycles of sputtering by Ar_{500}^+ clusters. The profiles of Fe, Ti, O and Sn are shown in Fig. 8. TiO_2 penetrated deep into the porous structure, as intended (and also observed for the as-

deposited sample in Fig. 3). Comparison of Fig. 3 and Fig. 8 shows that after 7 days immersion of a sample in 1 M H_2SO_4 the Ti concentration was somewhat diminished near the surface and the Fe concentration increased. However, the deposited TiO_2 is remarkably stable given the harsh acid treatment, which is in line with published literature [24].

Conclusions

Hematite layers, as obtained in this study by aerosol pyrolysis have non-negligible roughness and porosity. ALD was found successful in applying conformal TiO_2 capping with nominal layer thicknesses of 0.5, 2 and 7.5 nm, reaching deep into the porous hematite structure, as evidenced by XPS. HR-TEM confirmed that the capping TiO_2 layers were amorphous and conformal on the hematite films.

The photocurrents were strongly diminished as the TiO_2 capping layer thickness was increased. This clearly confirms that such coatings are most useful only when very thin - typically up to 1 nm thick layers - were employed. Post-calcination of as-deposited ALD films on hematite resulted in an increase of photocurrent, but only for an ALD thickness of 0.5 nm did the photocurrents exceed those of pristine hematite. This increase in photocurrents of annealed electrodes can be ascribed to the loss of the blocking function of TiO_2, probably due to increase in conductivity.

Exposure of uncovered films to 1 M sulfuric acid led to a nominal dissolution rate of 0.23 nm/h which was halved when a 7.5 nm thin capping TiO_2 layer was applied, showing the expected role of TiO_2 capping layer in the chemical protection of the photoanode. These layers possessed remarkable stability in such a highly acid environment, although the stability was limited for long exposure times.

Acknowledgements

The authors would like to thank the Czech Science Foundation (project number 20-11635S) for financial support, M. Paidar (UCT Prague) for ICP analysis and L. Hromadko (University Pardubice) for XRD analyses. The financial support of the Ministry of Education, Youth and Sports (MEYS) of the Czech Republic via projects NANOBIO (Reg. No Reg. No. CZ.02.1.01/0.0/0.0/17_048/0007421) and NPU I (LQ1601) is also acknowledged. The financial support of MEYS CR (LM2018110) for the FIB sample preparation and TEM analysis is acknowledged.

References

[1] M. Pourbaix, Atlas d'Equilibres Électrochimiques, Gauthier-Villars & Cie, Paris, 1963.
[2] R.L. Anderson, Experiments on Ge-GaAs heterojunctions, Solid State Electronics 5(1962) 341-351.
[3] T. Moehl, J. Suh, L. Sévery, R. Wick-Joliat, S.D. Tilley, Investigation of (Leaky) ALD TiO2 Protection Layers for Water-Splitting Photoelectrodes, ACS Applied Materials & Interfaces, 9 (2017) 43614-43622.
[4] T. Kotrla, Š. Paušová, M. Zlámal, M. Neumann-Spallart, J. Krýsa, Preparation of Sn-doped semiconducting Fe2O3 (hematite) layers by aerosol pyrolysis, Catalysis Today, 313 (2018) 2-5.
[5] J. Krýsa, T. Imrich, Š. Paušová, H. Krýsová, M. Neumann-Spallart, Hematite films by aerosol pyrolysis: Influence of substrate and photocorrosion suppression by TiO2 capping, Catalysis Today, 335 (2019) 418-422.
[6] S.M. George, Atomic Layer Deposition: An Overview, Chemical Reviews, 110 (2010) 111-131.
[7] M. Liu, C.-Y. Nam, C.T. Black, J. Kamcev, L. Zhang, Enhancing Water Splitting Activity and Chemical Stability of Zinc Oxide Nanowire Photoanodes with Ultrathin Titania Shells, The Journal of Physical Chemistry C, 117 (2013) 13396-13402.
[8] P.J. Reed, H. Mehrabi, Z.G. Schichtl, R.H. Coridan, Enhanced Electrochemical Stability of TiO2-Protected, Al-doped ZnO Transparent Conducting Oxide Synthesized by Atomic Layer Deposition, ACS Applied Materials & Interfaces, 10 (2018) 43691-43698.
[9] C. Li, T. Wang, Z. Luo, D. Zhang, J. Gong, Transparent ALD-grown Ta2O5 protective layer for highly stable ZnO photoelectrode in solar water splitting, Chemical Communications, 51 (2015) 7290-7293.
[10] X. Yang, R. Liu, C. Du, P. Dai, Z. Zheng, D. Wang, Improving Hematite-based Photoelectrochemical Water Splitting with Ultrathin TiO2 by Atomic Layer Deposition, ACS Applied Materials & Interfaces, 6 (2014) 12005-12011.
[11] X. Li, P.S. Bassi, P.P. Boix, Y. Fang, L.H. Wong, Revealing the Role of TiO2 Surface Treatment of Hematite Nanorods Photoanodes for Solar Water Splitting, ACS Applied Materials & Interfaces, 7 (2015) 16960-16966.
[12] M.G. Ahmed, I.E. Kretschmer, T.A. Kandiel, A.Y. Ahmed, F.A. Rashwan, D.W. Bahnemann, A Facile Surface Passivation of Hematite Photoanodes with TiO2 Overlayers for Efficient Solar Water Splitting, ACS Applied Materials & Interfaces, 7 (2015) 24053-24062.
[13] T.H. Jeon, G.-h. Moon, H. Park, W. Choi, Ultra-efficient and durable photoelectrochemical water oxidation using elaborately designed hematite nanorod arrays, Nano Energy, 39 (2017) 211-218.
[14] J. Wang, B. Feng, J. Su, L. Guo, Enhanced Bulk and Interfacial Charge Transfer Dynamics for Efficient Photoelectrochemical Water Splitting: The Case of Hematite Nanorod Arrays, ACS Applied Materials & Interfaces, 8 (2016) 23143-23150.
[15] S.B. Sadale, S.M. Chaqour, O. Gorochov, M. Neumann-Spallart, Photoelectrochemical and physical properties of tungsten trioxide films obtained by aerosol pyrolysis, Materials Research Bulletin, 43 (2008) 1472-1479.
[16] F. Dvorak, R. Zazpe, M. Krbal, H. Sopha, J. Prikryl, S. Ng, L. Hromadko, F. Bures, J.M. Macak, One-dimensional anodic TiO2 nanotubes coated by atomic layer deposition: Towards advanced applications, Applied Materials Today, 14 (2019) 1-20.
[17] P.S. Shinde, S.B. Sadale, P.S. Patil, P.N. Bhosale, A. Brüger, M. Neumann-Spallart, C.H. Bhosale, Properties of spray deposited titanium dioxide thin films and their application in photoelectrocatalysis, Solar Energy Materials and Solar Cells, 92 (2008) 283-290.
[18] M.J. Jackman, A.G. Thomas, C. Muryn, Photoelectron Spectroscopy Study of Stoichiometric and Reduced Anatase TiO2(101) Surfaces: The Effect of Subsurface Defects

on Water Adsorption at Near-Ambient Pressures, The Journal of Physical Chemistry C, 119 (2015) 13682-13690.
[19] N.S. McIntyre, D.G. Zetaruk, X-ray photoelectron spectroscopic studies of iron oxides, Analytical Chemistry, 49 (1977) 1521-1529.
[20] C. Sleigh, A.P. Pijpers, A. Jaspers, B. Coussens, R.J. Meier, On the determination of atomic charge via ESCA including application to organometallics, Journal of Electron Spectroscopy and Related Phenomena, 77 (1996) 41-57.
[21] J. Rodriguez-Pereira, J.H. Quintero-Orozco, R. Ospina, TiZrN thin films under CO2 and thermal treatment characterized by x-ray photoelectron spectroscopy, Surface Science Spectra, 26 (2019) 024013.
[22] D. Barreca, G. Carraro, A. Gasparotto, C. Maccato, M.E.A. Warwick, K. Kaunisto, C. Sada, S. Turner, Y. Gönüllü, T.-P. Ruoko, L. Borgese, E. Bontempi, G. Van Tendeloo, H. Lemmetyinen, S. Mathur, Fe2O3–TiO2 Nano-heterostructure Photoanodes for Highly Efficient Solar Water Oxidation, Advanced Materials Interfaces, 2 (2015) 1500313.
[23] G. Carraro, C. Maccato, A. Gasparotto, M.E.A. Warwick, C. Sada, S. Turner, A. Bazzo, T. Andreu, O. Pliekhova, D. Korte, U. Lavrenčič Štangar, G. Van Tendeloo, J.R. Morante, D. Barreca, Hematite-based nanocomposites for light-activated applications: Synergistic role of TiO2 and Au introduction, Solar Energy Materials and Solar Cells, 159 (2017) 456-466.
[24] G.C. Correa, B. Bao, N.C. Strandwitz, Chemical Stability of Titania and Alumina Thin Films Formed by Atomic Layer Deposition, ACS Applied Materials & Interfaces, 7 (2015) 14816-14821.